

Text-Printed Image: Bridging the Image-Text Modality Gap for Text-centric Training of Large Vision-Language Models

Shojiro Yamabe^{1,2,†} Futa Waseda^{1,3} Daiki Shiono^{1,4} Tsubasa Takahashi^{1,‡}
¹Turing Inc. ²Institute of Science Tokyo ³The University of Tokyo ⁴Tohoku University
[†]yamabe.s.2fb0@m.isct.ac.jp [‡]tsubasa.takahashi@turing-motors.com

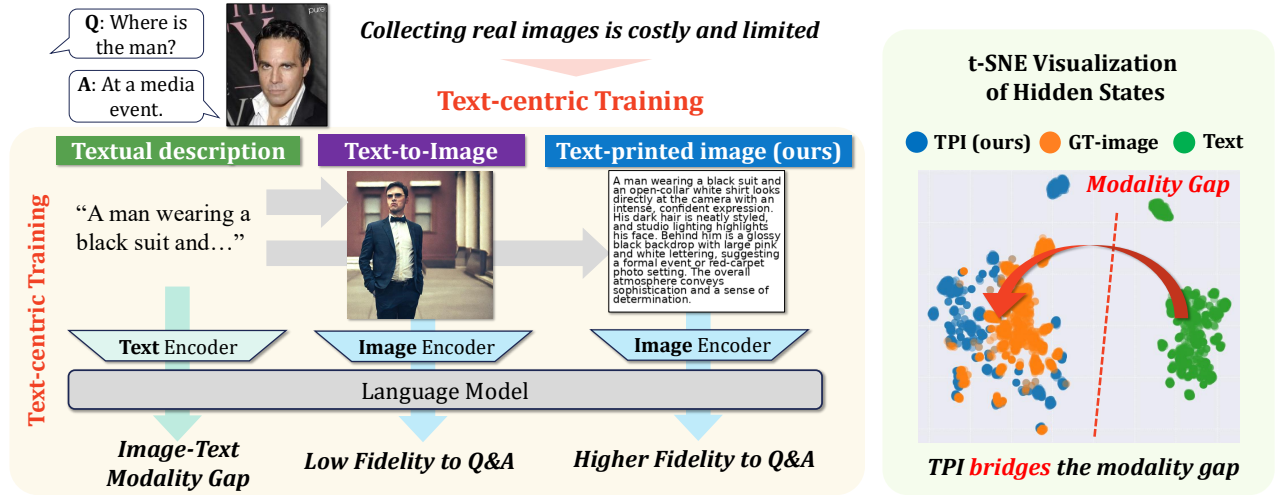


Figure 1. **Text-Printed Image (TPI)** provides an efficient and broadly applicable approach for text-centric training. While raw text input suffers from an image-text modality gap and synthetic images generated by a text-to-image model lose fidelity to Q&A pairs, TPI bridges this gap by embedding textual content into the visual pathway, achieving high fidelity to the ground-truth visual supervision.

Abstract

Recent large vision-language models (LVLMs) have been applied to diverse VQA tasks. However, achieving practical performance typically requires task-specific fine-tuning with large numbers of image-text pairs, which are costly to collect. In this work, we study text-centric training, a setting where only textual descriptions are available and no real images are provided, as a paradigm for low-cost data scaling. Unlike images, whose collection is often restricted by privacy constraints and scarcity in niche domains, text is widely available. Moreover, text is easily editable, enabling automatic diversification and expansion with LLMs at minimal human effort. While this offers clear advantages over image collection in terms of scalability and cost, training on raw text without images still yields limited gains on VQA tasks because of the image-text modality gap. To address this issue, we propose a **Text-Printed Image (TPI)**, which generates synthetic images by directly rendering the given textual description on a plain white canvas. This simple ren-

dering projects text into the image modality and can be integrated into arbitrary existing LVLM training pipelines at low cost. Moreover, TPI preserves the semantics of the text, whereas text-to-image models often fail to do. Across four models and seven benchmarks, our systematic experiments show that TPI enables more effective text-centric training than synthetic images generated by a diffusion model. We further explore TPI as a low-cost data-augmentation strategy and demonstrate its practical utility. Overall, our findings highlight the significant potential of text-centric training and, more broadly, chart a path toward fully automated data generation for LVLMs.

1. Introduction

Large Vision-Language Models (LVLMs) [38] have emerged as a powerful extension of Large Language Models (LLMs). Building on strong foundational capabilities, they have been applied across diverse VQA tasks, includ-

ing autonomous driving [72] and healthcare [21]. To attain practical performance on these downstream tasks, task-specific fine-tuning is typically required.

However, constructing a large-scale dataset remains challenging for such training, as practical SFT typically requires vast amounts of image–text instructions [38, 61, 62]. In contrast to LLM training, which benefits from abundant text corpora [5], LVLM training requires image-conditioned instruction data, and constructing such data is substantially more costly [31, 38]. Although automated methods for scraping web images and pairing them with corresponding text have been proposed [10, 12, 30, 52, 67], their applicability is often limited in specialized or niche domains [32, 51].

In this work, we consider *text-centric training*, where only textual descriptions are available and no images are provided. Our premise is that text is abundant and easy to prepare compared to images. Rich text corpora and structured lexical resources make it possible to synthesize descriptions from class names and concept taxonomies [16, 20, 58]. Moreover, text is much easier to modify than images. While changing a small detail in an image is difficult [22], textual descriptions can be edited or expanded with little effort, and LLMs can automatically generate diverse variants [57]. Recent advances in LLM-based data augmentation [13, 56] further enhance this potential, enabling scalable and diverse text synthesis at low cost. Taken together, these factors make text-centric training a promising yet underexplored direction for advancing LVLMs when images are scarce or unavailable.

A primary challenge for effective text-centric training is the *image-text modality gap* [17, 35, 66, 68], which is a mismatch between the latent distributions of textual and visual representations within a model. Because of this gap, training only on given raw text fails to generalize effectively to visual inputs, as the representations learned from text differ from those required to process images during inference.

A straightforward approach to bridge this gap is to synthesize images using text-to-image models (T2I), such as diffusion models [45]; however, T2I often struggles to maintain fidelity to the given textual descriptions [23, 25]. The generated images often deviate from the intended semantic content, making them unsuitable as training data. Indeed, our experimental results confirm that T2I-generated images are poorly relevant to their corresponding queries and responses, leading to suboptimal performance. Mitigating this issue typically requires extensive sampling and manual verification, which substantially increases costs.

To bridge the modality gap while maintaining semantic fidelity, we propose a low-cost yet effective method, *Text-Printed Image (TPI)*. Given a textual description, TPI renders the text onto a plain white canvas and uses the resulting image as the visual input during training. This de-

sign ensures that the LVLM receives the full semantics of the text while the image encoder still processes it in the visual modality, thereby preserving semantic fidelity and mitigating the modality gap. In our experiments, TPI-based training outperforms training on T2I-generated images and matches or approaches the performance achieved with ground-truth images on several datasets. Furthermore, TPI can be applied without a GPU, and it is architecture-agnostic because it requires no changes to the training pipeline. Overall, the combination of low cost and strong effectiveness makes TPI a highly practical approach for LVLM training.

Finally, we introduce a data augmentation approach based on TPI. We automatically generate synthetic textual descriptions by using an LLM and evaluate models trained on this data. Even when seeding the augmentation with only 1% of the original dataset, we can observe measurable performance gains. Moreover, augmenting the full training set with the synthetic text yields additional gains over the model trained only on the full dataset. These results reinforce that text-centric training with TPI is a promising direction for low-cost automatic training data generation for LVLMs.

Contributions. Our contributions are summarized as:

- We introduce a light-weight and architecture-agnostic text-centric training method, *Text-Printed Image (TPI)*, that bridges the modality gap while preserving text semantics by rendering textual descriptions as images.
- We conduct extensive evaluations over multiple LVLMs and downstream tasks, showing that training with TPI can outperform training with T2I-generated images and, on some benchmarks, match or closely approach training with ground-truth images.
- We investigate a practical text-driven augmentation that leverages LLMs to generate instruction data, showing that TPI enables performance improvements even with only 1% of the original dataset.

2. Related works

2.1. Large Vision-Language Models

LVLMs are a family of models built on LLMs that interpret not only language but also visual information [3, 7, 11, 36, 38, 49, 54, 55, 76, 77]. These models are typically trained on paired image–text data. While these models exhibit strong general-purpose capabilities, they typically require large amounts of training data. In this work, we focus on LVLMs with this architecture and study text-centric training to mitigate data scarcity.

2.2. Text-centric training

CLIP-based approach. Prior work has explored text-centric training and proposed methods to reduce the modal-

ity gap [33, 35, 44, 46, 63, 66, 68, 73, 74]. However, they are designed for CLIP-style dual encoders and do not transfer directly to LVLMs. Specifically, while they assume a one-to-one match between image and text representation dimensions, this assumption does not hold for LVLMs because text representations are token-based and their dimensionality changes with the length of the input text.

T2I-based approach. Several approaches use T2I to generate synthetic images from given descriptions [1, 2, 4, 16, 18, 34, 50, 58–60]. However, as demonstrated in our experiments, T2I-generated images struggle to reflect the given text faithfully, and training on them does not yield sufficient performance improvements. Moreover, obtaining high-quality images requires substantial trial-and-error and quality checks, making the process costly.

Text-centric training for LVLMs. Recent works focus on text-centric training for LVLMs [8, 14, 24, 64]. Some of them [14, 24] showed that training LVLMs solely on text, analogous to LLM training, can improve their reasoning ability. Although applications to VQA tasks have been explored [8], the gains remain limited due to the image–text modality gap, as our experiments later demonstrate. Yu et al. [64] proposed to mitigate this gap by adding a constant vector to the text features. However, similar to CLIP-based approaches, their method assumes that image and text features have the same dimensionality, which makes it difficult to apply to many existing LVLMs. In addition, the constant vector must be added not only during training but also at inference time, incurring extra inference cost. In this work, we propose an architecture-agnostic and low-cost training method for VQA tasks that mitigates this gap without any inference-time modifications.

2.3. Other synthetic data generation approaches

To enable scalable training, many studies have explored synthetic data generation that is not text-centric. A common strategy leverages existing image sources [6, 10, 12, 26, 28–30, 52, 53, 67, 69, 70, 75]. These methods construct synthetic datasets by collecting images from the web or other corpora and attaching high-quality captions. However, they face an inherent limitation: applicability diminishes when publicly available images are scarce, particularly in specialized domains. Although this line of work is important, our work focuses on text-centric training. Consequently, methods that rely on sourcing images to synthesize datasets fall outside the scope of this paper.

3. Method

We propose TPI for effective text-centric training, where only textual descriptions are available. Preparing text is easier than images: Text is abundant and can be assembled from concept resources such as taxonomies or class

names [16, 20, 58], and diverse variants can be generated automatically with LLMs at minimal human cost [13, 56]. However, effective training remains challenging due to the image–text modality gap. To address this issue, we investigate how to learn effectively from given textual descriptions and introduce a method that enables effective training.

3.1. Problem Formulation

Notation. Recent LVLMs, such as LLaVA [38] and Qwen-VL [3, 54], typically consist of a vision encoder, a projector, and an LLM. Given an image–query pair (i, q) , the model divides the image into patches and projects them into image features $v = p_\theta(i)$, where $p_\theta(\cdot)$ denotes the image processor composed of the vision encoder and the projector. The image features are then fed into the LLM $f_\phi(\cdot)$, resulting in the conditional distribution for response r :

$$f_\phi(r \mid p_\theta(i), q). \quad (1)$$

Text-centric training. In text-centric training, the image i is unavailable; instead, only a textual description t is given. We introduce a transformation T that synthesizes features directly from text. Given a training dataset \mathcal{D}_{txt} consisting of triplets (t, q, r) , the objective is formulated as:

$$\mathcal{L}(\theta, \phi) = \mathbb{E}_{(t, q, r) \sim \mathcal{D}_{\text{txt}}} [-\log f_\phi(r \mid T(t), q)]. \quad (2)$$

For instance, if T is the text encoder of the LLM, the model is trained using raw text in the same way as a standard LLM. Alternatively, if T is composed of a T2I generator G and the image processor, such as $T(t) = p_\theta(G(t))$, it means that the training uses synthetic images created by the generator G from text t .

3.2. Difficulty and Requirements

The main difficulty in effective text-centric training is the *image–text modality gap*, an inherent bias of the vision encoder whereby image features projected by the vision encoder and text features lie in systematically different regions of the representation space [17, 35, 63, 66, 68]. As a result, even when an image and its textual description express the same semantics, the LVLM can interpret them as disparate signals, so the effectiveness of learning from raw text alone remains limited. Thus, it is desirable that the synthesized feature $s = T(t)$ aligns with the image feature $v_t = f_\theta(i_t)$, where i_t denotes a hypothetical image that visually represents the textual description t .

In addition, to design a practical solution, we require the transformation T to satisfy the following three criteria:

(R1) Compatibility with pretrained LVLMs: To ensure applicability to a broad range of LVLMs, the transformation T should not rely on assumptions about model architecture or the visual encoding pipeline. CLIP-based methods [35, 46, 63, 64, 68] that assume alignment between text

and image feature dimensions cannot be applied to most LVLMs because their text feature dimensions vary with the input length. Thus, alternative architecture-agnostic approaches are needed for LVLMs.

(R2) Preservation of text semantics: To maintain data quality, the synthesized feature $s = T(t)$ should faithfully preserve the semantics of the given text t . T2I-generated images often fail to faithfully follow the provided text, leading to inconsistencies with the paired query and response.

(R3) Efficiency and scalability: To preserve the low-cost advantage of text-centric training, T should be computationally efficient and scalable. Additional training of T or reliance on expensive text-to-image synthesis pipelines limit scalability. T2I are resource-intensive and often require domain-specific fine-tuning, undermining this efficiency advantage.

3.3. Text-Printed Images

To address the difficulty and satisfy the above requirements, we introduce *TPI* that renders the given textual description directly onto a plain white canvas (Figure 1). Our key insight is that, by directly rendering the provided text, TPI is processed by the vision encoder before reaching the LLM, while preserving its complete semantics. The routing is crucial: the modality gap originates from biases and mismatches induced by the image encoder, so addressing this issue requires leveraging representations obtained from the image encoder. At the same time, TPI preserves the full semantics of the description since the image explicitly contains the original text. It satisfies the requirement of semantic fidelity (R2).

Formally, let $R(\cdot; \psi)$ be a deterministic renderer that maps text to an RGB image with layout parameters ψ , such as font size and image size. The transformation is:

$$T_{\text{print}}(c_i) = p_{\theta}(R(c_i; \psi)). \quad (3)$$

We summarize how TPI compares with previous approaches against the above requirements in Table 1 and find that TPI satisfies (R1–R3). For **(R1)**, TPI uses the unmodified visual pathway: the synthesized image is processed by the existing image encoder and projector, without retraining of the projector or LLM, yielding a true drop-in replacement in standard training code. For **(R2)**, as mentioned above, a TPI is generated by directly rendering the textual description t onto an image, thus faithfully preserving its semantics. We empirically validate this in Section 4.4.2. For **(R3)**, TPI relies solely on a deterministic, training-free renderer R and can be executed extremely efficiently, maintaining a clear cost advantage over text-to-image baselines, achieving roughly three orders of magnitude higher throughput as shown in Section 4.4.4. Together, TPI provides a practical and scalable way to realize effective text-centric training for existing LVLMs.

Table 1. Comparison of text-centric training methods.

Method	Modality Gap Reduction	(R1) Compatibility	(R2) Semantic fidelity	(R3) Efficiency
Text-only		✓	✓	✓
CLIP-based	✓		✓	✓
Text-to-Image	✓	✓		
TPI (ours)	✓	✓	✓	✓

4. Experiments

We evaluate the effectiveness of TPI when synthetic textual descriptions are available from three perspectives:

- (i) *How closely can TPI training approach image-based training in downstream performance?* (Section 4.2): We train models using textual descriptions derived from ground-truth images and compare them with models trained directly on the ground-truth images.
- (ii) *How does training with TPI change model behavior?* (Section 4.3): We analyze the behaviors of trained models in depth by comparing the output distributions and internal representations.
- (iii) *What factors enable effective learning with TPI?* (Section 4.4): We conduct various analyses to characterize when and why TPI training works.

4.1. Experimental Setup

Datasets. We use the following three types of datasets:

1. *General VQA:* We use three commonly used datasets: ScienceQA [40], OK-VQA [40], and VizWiz [19].
2. *Text VQA:* We also use three datasets that utilize images containing text: ChartQA [41], InfoVQA [43], and DocVQA [42]. These tasks contain images like charts and posters that are difficult to represent with text alone.
3. *Domain-specific VQA:* To test whether TPI training transfers to unseen domains, we use DriveLM [47], a VQA dataset for autonomous driving. It contains vehicle-view images and corresponding questions.

For General VQA and Text VQA, we evaluate performance using the lmms-eval library [65]. For DriveLM, we follow the official implementation and adopt evaluation by GPT-4.

TPI Generation Settings. For a fair comparison with image-based training, we first automatically generate textual descriptions from each ground-truth image using Qwen2.5-VL-32B [54]. We simply provide the model with an image and a question to generate an image description. We note that the GT images are used solely to generate textual descriptions and are not required for practical use. For each description, we render text using Python and the Pillow library [9]. Each TPI is an RGB image of size 336×336 px with a white background and black text. The font size is capped at 32 pt and is downsampled as needed to fit within the canvas (see Appendix B for details).

Models and Training Setup. We use four LVLMs: LLaVA1.5 7B/13B [38], Qwen2.5 VL 7B Instruct [54], and

Table 2. **TPI (ours) overcomes the image-text modality gap and achieves superior performance.** *Text-only* offers only limited gains due to the gap. Each value represents the test score obtained after fine-tuning the pretrained model on the training set of each task.

Model	Training	Tasks							Avg.
		ScienceQA	OK-VQA	VizWiz	ChartQA	InfoVQA	DocVQA	DriveLM	
LLaVA 7B	Pretrained	66.09	49.87	52.89	17.12	21.91	23.86	47.84	39.94
	Text-only	72.63	60.73	59.25	19.24	25.36	28.61	64.03	47.12
	Text-to-Image	75.01	61.16	64.14	18.88	26.02	25.18	68.61	48.43
	Text-printed Image (Ours)	75.11	61.70	61.96	23.28	28.43	33.80	65.49	49.97
	GT-Image (Oracle)	78.78	62.12	67.56	36.68	29.81	39.93	74.20	55.58
LLaVA 13B	Pretrained	71.39	52.49	56.33	19.32	25.87	27.86	51.93	43.60
	Text-only	75.61	64.59	63.79	24.32	29.21	32.85	64.50	50.70
	Text-to-Image	76.15	63.84	64.67	21.04	29.76	27.80	69.62	50.41
	Text-printed Image (Ours)	76.30	64.73	64.46	28.72	30.75	36.70	64.00	52.24
	GT-Image (Oracle)	80.12	64.53	66.96	40.28	33.73	43.07	74.86	57.65
Qwen2.5 VL	Pretrained	76.65	43.88	70.80	83.28	80.21	94.36	39.49	69.81
	Text-only	86.53	61.78	68.54	85.92	77.60	92.89	66.26	77.07
	Text-to-Image	88.20	60.61	66.45	70.08	70.64	79.75	71.55	72.47
	Text-printed Image (Ours)	90.43	62.24	68.59	86.24	77.61	93.38	67.09	77.94
	GT-Image (Oracle)	93.51	61.63	70.54	86.76	78.77	93.89	75.16	80.04
LLaMA Vision	Pretrained	50.77	25.99	58.32	22.28	46.98	80.83	34.33	45.64
	Text-only	66.91	48.28	62.19	46.68	60.51	83.38	41.56	58.50
	Text-to-Image	86.81	61.18	67.96	39.04	52.34	66.78	48.44	60.36
	Text-printed Image (Ours)	90.93	62.65	70.44	73.28	65.36	90.84	52.37	72.27
	GT-Image (Oracle)	93.65	63.04	72.32	76.48	67.90	92.47	55.16	74.43

Llama 3.2 11B Vision [15]. All models are fine-tuned with LoRA. Detailed setups are in Appendix A.2.

Baselines. We use three baselines for comparison: (i) *Text-only training*, which directly uses the given textual description as training data. (ii) *Text-to-Image (T2I)*, which involves generating images from the textual descriptions using T2I model and then using those images for training. We use Stable Diffusion XL 1.0 [45] as T2I model. We sample with 25 denoising steps and a guidance scale of 5.0. (iii) *Ground-Truth Image (GT-Image, Oracle)*, which uses the originally paired image for each text for training, as a performance upper bound.

4.2. Downstream Performance Improvement

We first evaluate training effectiveness using benchmark scores. The results in Table 2 show that (i) the modality gap exists in text-only training, and (ii) TPI reduces this gap and improves performance.

Modality gap. The results for LLaVA 7B/13B and LLaMA Vision show significant performance differences between *Text-only* and *GT-Image*, supporting that the improvements from text-only training are fundamentally constrained by the image-text modality gap. Although the loss decreased during text-only training, trained models fail to

handle image inputs effectively at test time. In contrast, for Qwen VL, the performance difference between *Text-only* and *GT-Image* is not substantial. We attribute this to Qwen’s higher intrinsic performance, which makes the gap less apparent and potentially a lower bias in its image encoder.

Effectiveness of TPI. TPI outperforms baseline methods, indicating that it effectively mitigates the modality gap while preserving semantic fidelity. Across all models, TPI clearly exceeds *Text-only* and, on some tasks, approaches *GT-Image*. *T2I* in particular underperforms on Text VQA, which is consistent with prior findings [34]. We attribute this to the difficulty of diffusion models in generating images that faithfully reflect the given text. We provide a detailed quantitative evaluation for faithfulness in Section 4.4.

4.3. Model Behavior Analyses

To understand how TPI affects model behavior, we compare a model trained on *GT-Image* with one trained on TPI.

4.3.1. Output Distribution Comparison

We assess similarity between output distributions using the JS divergence for each task’s test split to clarify behavioral differences that accuracy may obscure. As shown in Figure 2, TPI yields smaller divergences than the baselines, indicating effective training also at the level of output distribu-

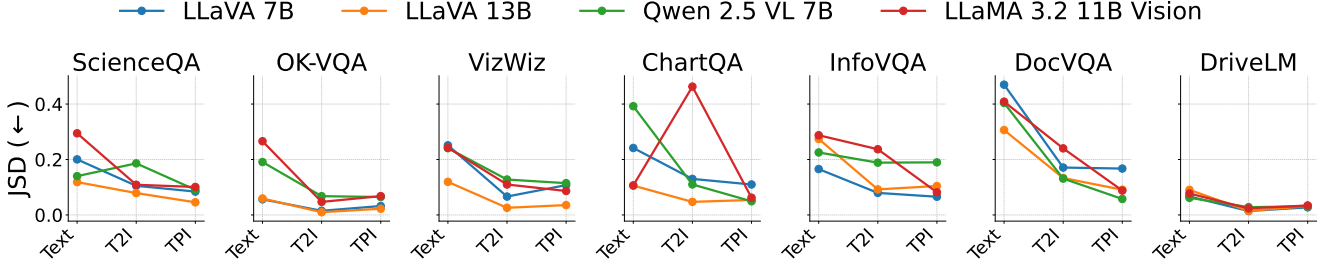


Figure 2. **TPI training yields output distributions most similar to models trained on GT-Images.** We compare the similarity to the model trained on *GT-Image* in output distributions. Each value represents the JS divergence on the test split.

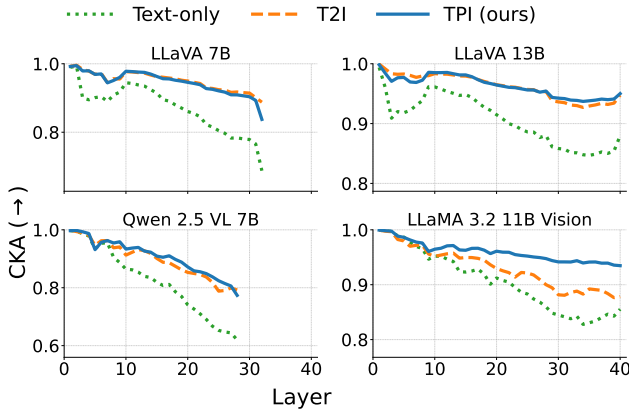


Figure 3. **Text-only training causes substantial drift in intermediate representations, while TPI mitigates it.** We compare the similarity to the model trained on *GT-Image* in intermediate representations by computing the layer-wise CKA.

tions. In contrast, *Text-only* exhibits consistently higher JS divergence, suggesting that training without images alters model behavior, even when downstream task scores may appear reasonable. *T2I* shows notably lower similarity on Text VQA, which is consistent with the results in Table 2.

4.3.2. Intermediate Representation Comparison

To examine how training inputs alter internal behavior, we compare intermediate representations. For each task’s test split, we extract the hidden state at the *last token* position and compute *Centered Kernel Alignment (CKA)* [27], which quantifies similarity between representation matrices, layer by layer. We report the average value across all tasks.

As shown in Figure 3, *Text-only* induces substantially larger shifts in intermediate representations compared with *T2I* and *TPI*. Notably, while performance improvements by *Text-only* are comparable to *GT-Image* for Qwen VL in Table 2, the drift in intermediate representations is pronounced. This suggests that training without images can alter behaviors and representations in ways that benchmark scores alone fails to capture. In contrast, *TPI* mitigates this drift and better preserves the geometric structure of hidden states learned from the original visual modality.

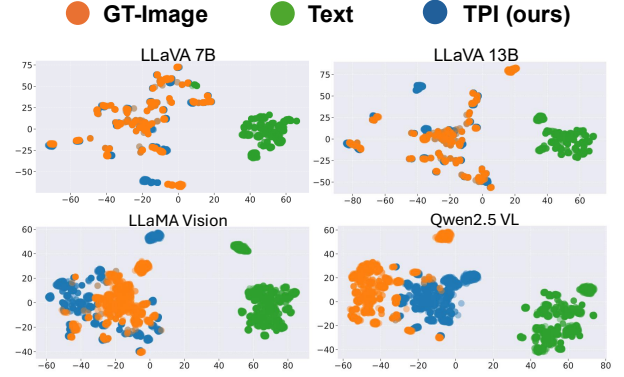


Figure 4. **TPI reduces the image-text modality gap.** We visualize t-SNE embeddings of intermediate features. While *Text-only* produces a large separation from image features, *TPI* aligns more closely with the visual manifold.

4.4. Analysis of TPI Effectiveness

4.4.1. t-SNE Visualization of the Modality Gap

To further investigate whether *TPI* effectively mitigates the image-text modality gap, we visualize the latent feature distributions. We feed the training examples into the pretrained model, extract the intermediate representations at the final token, and then apply t-SNE to these features.

Figure 4 shows the results in the ScienceQA task. The representations of *GT-Image* and *TPI* are closely located in the same region of the feature space, while *Text-only* form a clearly separated cluster. These qualitative results support our claim that *TPI* effectively bridges the modality gap by projecting textual information into the image modality.

4.4.2. Relevance Score Evaluation

To evaluate how *TPI* preserves given text semantics, we compute the relevance between synthetic images and their paired questions and answers. Following VQAScore [37], we define a **RELEVANCE SCORE** as a probability that measures the consistency:

$$\Pr\left(\text{“Yes”} \mid \text{image, “Is the image relevant to the following Question and Answer? Please answer Yes or No.”}\right).$$

Table 3. **Although T2I often fails to follow the provided prompts faithfully, TPI maintains high relevance.** We compute the Relevance Score, which measures how well each image aligns with the corresponding paired query and response.

Dataset	GT-Img.	T2I	TPI (ours)
ScienceQA	70.15	34.75 (49.5%)	57.32 (81.7%)
OK-VQA	69.27	54.38 (78.5%)	55.08 (79.5%)
VizWiz	65.79	44.49 (67.6%)	54.92 (83.5%)
ChartQA	79.22	20.78 (26.2%)	89.01 (112.4%)
InfoVQA	80.13	21.07 (26.3%)	80.53 (100.5%)
DocVQA	94.02	21.93 (23.3%)	79.54 (84.6%)
DriveLM	31.91	29.75 (93.2%)	29.55 (92.6%)
Avg.	70.07	32.45 (46.3%)	63.61 (90.8%)

Table 4. **Relationship between OCR capability and the effectiveness of TPI.** Gap Ratio represents the fraction of *GT-Img.* gains that TPI training recovers.

	OCRBench	TextVQA	Gap Ratio
LLaVA 7B	20.3	47.9	64%
LLaVA 13B	22.6	52.8	61%
Qwen2.5 VL	83.7	82.9	79%
Llama Vision	75.2	73.4	92%

A higher score indicates stronger alignment between the image and QA. We compute the score using Qwen2.5-VL-32B [54], a sufficiently trained model.

As shown in Table 3, the relevance scores of TPI are higher than those for T2I. This confirms our claim that TPI can preserve text semantics while T2I often struggles to remain faithful to the text, and the generated images can include elements that conflict with the QA.

4.4.3. Impact of OCR Ability on TPI Effectiveness

Since interpreting TPI requires recognizing text embedded in images, we examine how OCR capability relates to effectiveness. We assess OCR ability using *OCRBench* [39] and *TextVQA* [48]. We quantify the effectiveness of TPI training by computing the Gap Ratio (GR): $\frac{\text{TPI} - \text{Pretrained}}{\text{GT} - \text{Img.} - \text{Pretrained}}$. We report the average score across all tasks.

Table 4 shows that models with higher OCR scores tend to exhibit larger GRs, indicating OCR ability correlates with TPI effectiveness. Although Qwen attains the highest OCR score, its strong *Pretrained* baseline makes the denominator ($\text{GT} - \text{Img.} - \text{Pretrained}$) small, yielding a lower GR. These observations suggest that models with at least moderate OCR ability benefit more from TPI. Nevertheless, TPI still outperforms *Text-only* even for LLaVA-7B/13B, demonstrating that TPI can be effective even when OCR ability is limited.

Table 5. Image generation time for 6,218 descriptions.

Method	Total time [s]	Images per second
T2I (1 H100 GPU)	39347	0.16
TPI (CPU-only, ours)	40	154.40

4.4.4. Image generation efficiency

To compare the computational cost of data construction, we measure the wall-clock time required to generate images. For TPI, we use Intel Xeon Platinum 8480+ CPUs (32 cores, 64 threads), and for T2I, we use a single NVIDIA H100 GPU. Table 5 reports the results on 6,218 ScienceQA images: T2I takes 10.9 hours, whereas TPI finishes in 40.27 seconds. This result indicates that TPI enables substantially faster data construction without any GPU, making it a practical choice for large-scale text-centric training.

5. Text-Centric Data Augmentation at Scale

We present an exploratory study toward scalable text-centric training. We augment textual description at scale by using an LLM and then train with TPI. We examine two regimes: (i) a low-resource setting, where only a small seed subset is available, to test whether LLM-augmented descriptions with TPI improve over the pretrained model; and (ii) a full-data setting, where the entire training set is available, to assess whether the same augmentation still yields gains over a baseline trained on the full original dataset.

5.1. Augmentation Methods Setup

We adapt an established augmentation method for LLMs [56] to the data generation for LVLMs with minimal modifications. From a given initial data pool, we randomly select eight demonstrations, which consist of a query, response, and description. We then provide them to the LLM to generate one new sample. The new sample is added to the data pool, and the procedure is repeated. We first generate 10,000 samples, then compute ROUGE-L against the existing dataset and filter out highly similar items with scores ≥ 0.8 . We use GPT-4o-mini for generation, and the training setup is identical to Section 4. For details on data generation, see Appendix C.

5.2. Augmentation from Small Dataset

To simulate data-scarce conditions, we use 1% and 10% subsets of the original dataset as the initial data pool. For training, we use a mixed dataset that combines the original subset with the synthesized data. Results in Table 6 show that the performance of the trained model with the synthesized dataset exceeds that of the pretrained models. It suggests that augmentation via TPI is effective. A particularly notable performance improvement was observed on OK-VQA. This is likely because OK-VQA is a task that depends on external knowledge, and data augmentation may

Table 6. Performance of data augmentation with a small amount of original data via text-centric training.

	Methods	Models			
		LLaVA 7B	LLaVA 13B	Qwen	LLaMA
ScienceQA	Pretrained	66.09	71.39	76.65	50.77
	Orig. (1%)				
	+ Text-only	65.44	70.15	86.96	66.04
	+ T2I	64.01	<u>71.05</u>	<u>86.81</u>	87.36
	+ TPI (Ours)	<u>64.20</u>	70.40	88.25	<u>86.96</u>
	Orig. (10%)				
	+ Text-only	62.02	71.24	88.15	75.21
	+ T2I	69.36	<u>72.78</u>	<u>89.94</u>	<u>89.29</u>
	+ TPI (Ours)	<u>68.57</u>	73.28	90.33	89.39
	Pretrained	49.87	52.49	43.88	25.99
OK-VQA	Orig. (1%)				
	+ Text-only	<u>55.03</u>	<u>58.05</u>	60.28	34.95
	+ T2I	52.00	55.87	<u>59.07</u>	<u>54.09</u>
	+ TPI (Ours)	55.62	61.04	61.94	57.23
	Orig. (10%)				
	+ Text-only	57.85	62.03	63.19	42.46
	+ T2I	<u>58.78</u>	<u>62.52</u>	62.07	<u>59.66</u>
	+ TPI (Ours)	60.26	64.26	<u>62.81</u>	60.18

have enabled the LLM to synthesize new data containing novel knowledge that is not included in the original subset. Furthermore, in a comparison to baselines, TPI shows the greatest performance increase under most conditions, which is consistent with our earlier analyses in Section 4 and supports the high quality of TPI as a training signal.

5.3. Additional Augmentation from Full Dataset

Next, we investigate whether TPI can achieve further performance improvements in a scenario where the full training dataset is available. Results are shown in Table 7. For ScienceQA, we observe up to about a 2-point increase, indicating that augmentation with TPI can still contribute even in near-saturation regimes. In contrast, the improvement on OK-VQA is small. This might be because the full dataset already contains a sufficiently diverse range of external knowledge, and the LLM was unable to generate enough supplementary synthetic data to complement it.

Remark. The significance of this experiment lies not only in demonstrating score improvements but in illustrating a promising direction for low-cost and practical data augmentation. There is still significant room for development in data augmentation based on text-centric training. The augmentation method used in this experiment is a minimal adaptation of an existing method for LLMs. Thus, further improvements can be expected by developing methods specifically designed for text-centric training in LVLMs.

Table 7. Performance of data augmentation with full original data via text-centric training.

	Methods	Models			
		LLaVA 7B	LLaVA 13B	Qwen	LLaMA
ScienceQA	Orig. (100%)	78.78	80.12	93.51	93.65
	+ Text-only	71.15	74.47	90.48	85.67
	+ T2I	<u>79.47</u>	81.80	<u>94.99</u>	<u>94.15</u>
	+ TPI (Ours)	80.27	<u>81.66</u>	95.49	94.60
OK-VQA	Orig. (100%)	62.12	64.53	61.63	63.04
	+ Text-only	60.29	64.02	63.70	51.30
	+ T2I	<u>61.05</u>	<u>64.55</u>	62.13	63.48
	+ TPI (Ours)	61.21	64.56	<u>62.55</u>	<u>63.38</u>

6. Discussion and Limitation

Generation setting of TPI. We conduct an extensive ablation on layout parameters, including font size, image resolution, and caption-generation method in Appendix D. We did not observe substantial performance differences across these ablations. This suggests that, for learning, what matters is the semantics of the text rendered in the TPI rather than its typographic style or layout.

Limitation. Our approach assumes that trained LVLMs possess certain visual understanding capabilities. Because TPI provides properties such as shape and color only as text, a model that has not already acquired those visual concepts cannot reliably learn them from TPI alone. Also, TPI requires a minimum level of OCR ability. In this sense, TPI implicitly assumes a setting where we start from a foundation model with broad visual knowledge and aim to specialize it toward task-specific capabilities, rather than teaching entirely new visual concepts from scratch. However, given that such foundation models are becoming increasingly common, TPI is a promising low-cost and effective solution for text-centric training.

7. Conclusion

We introduce TPI for effective text-centric training. TPI is lightweight and can be applied to a broad range of LVLm training pipelines without modification. Our experiments show that TPI mitigates the image-text modality gap through multiple evaluations, including benchmark improvements, alignment of internal representations, and visualization analyses. We further demonstrate that TPI offers better practical utility, such as preserving semantics, than T2I by comparing QA relevance and generation cost. Finally, we apply TPI to a data augmentation scenario and demonstrate that it further improves performance. Overall, our findings highlight TPI as a promising path toward scalable training for LVLms.

References

- [1] Hossein Aboutaleb, Hwanjun Song, Yusheng Xie, Arshit Gupta, Lijia Sun, Hang Su, Igor Shalymov, Nikolaos Pappas, Siffi Singh, and Saab Mansour. Magid: An automated pipeline for generating synthetic multi-modal datasets. In *Proceedings of the 2024 Conference of the North American Chapter of the Association for Computational Linguistics: Human Language Technologies (Volume 1: Long Papers)*, pages 5150–5167, 2024. 3
- [2] Pooria Ashrafi, Milad Yazdani, Moein Heidari, Dena Shahriari, and Ilker Hacihaliloglu. Vision-language synthetic data enhances echocardiography downstream tasks. *arXiv preprint arXiv:2403.19880*, 2024. 3
- [3] Jinze Bai, Shuai Bai, Shusheng Yang, Shijie Wang, Sinan Tan, Peng Wang, Junyang Lin, Chang Zhou, and Jingren Zhou. Qwen-vl: A versatile vision-language model for understanding, localization, text reading, and beyond, 2023. 2, 3
- [4] Assaf Ben-Kish, Moran Yanuka, Morris Alper, Raja Giryes, and Hadar Averbuch-Elor. Mitigating open-vocabulary caption hallucinations. In *Proceedings of the 2024 Conference on Empirical Methods in Natural Language Processing*, pages 22680–22698, 2024. 3
- [5] Tom Brown, Benjamin Mann, Nick Ryder, Melanie Subbiah, Jared D Kaplan, Prafulla Dhariwal, Arvind Neelakantan, Pranav Shyam, Girish Sastry, Amanda Askell, et al. Language models are few-shot learners. *Advances in neural information processing systems*, 33:1877–1901, 2020. 2
- [6] Guiming Hardy Chen, Shunian Chen, Ruifei Zhang, Junying Chen, Xiangbo Wu, Zhiyi Zhang, Zhihong Chen, Jianquan Li, Xiang Wan, and Benyou Wang. Allava: Harnessing gpt4v-synthesized data for lite vision-language models. *arXiv preprint arXiv:2402.11684*, 2024. 3
- [7] Zhe Chen, Jiannan Wu, Wenhai Wang, Weijie Su, Guo Chen, Sen Xing, Muyan Zhong, Qinglong Zhang, Xizhou Zhu, Lewei Lu, et al. Internvl: Scaling up vision foundation models and aligning for generic visual-linguistic tasks. In *Proceedings of the IEEE/CVF conference on computer vision and pattern recognition*, pages 24185–24198, 2024. 2
- [8] Dasol Choi, Guijin Son, Soo Yong Kim, Gio Paik, and Seunghyeok Hong. Improving fine-grained visual understanding in vlms through text-only training. *arXiv preprint arXiv:2412.12940*, 2024. 3
- [9] Alex Clark. Pillow (pil fork) documentation, 2015. 4, 2
- [10] Muzhi Dai, Jiashuo Sun, Zhiyuan Zhao, Shixuan Liu, Rui Li, Junyu Gao, and Xuelong Li. From captions to rewards (carevl): Leveraging large language model experts for enhanced reward modeling in large vision-language models. *arXiv preprint arXiv:2503.06260*, 2025. 2, 3
- [11] Wenliang Dai, Junnan Li, Dongxu Li, Anthony Tiong, Junqi Zhao, Weisheng Wang, Boyang Li, Pascale N Fung, and Steven Hoi. Instructblip: Towards general-purpose vision-language models with instruction tuning. *Advances in neural information processing systems*, 36:49250–49267, 2023. 2
- [12] Yihe Deng, Pan Lu, Fan Yin, Ziniu Hu, Sheng Shen, Quanquan Gu, James Y Zou, Kai-Wei Chang, and Wei Wang. Enhancing large vision language models with self-training on image comprehension. *Advances in Neural Information Processing Systems*, 37:131369–131397, 2024. 2, 3
- [13] Bosheng Ding, Chengwei Qin, Ruochen Zhao, Tianze Luo, Xinze Li, Guizhen Chen, Wenhan Xia, Junjie Hu, Anh Tuan Luu, and Shafiq Joty. Data augmentation using llms: Data perspectives, learning paradigms and challenges. In *ACL (Findings)*, 2024. 2, 3
- [14] Yifan Du, Zikang Liu, Yifan Li, Wayne Xin Zhao, Yuqi Huo, Bingning Wang, Weipeng Chen, Zheng Liu, Zhongyuan Wang, and Ji-Rong Wen. Virgo: A preliminary exploration on reproducing o1-like mllm. *arXiv preprint arXiv:2501.01904*, 2025. 3
- [15] Abhimanyu Dubey, Abhinav Jauhri, Abhinav Pandey, Abhishek Kadian, Ahmad Al-Dahle, Aiesha Letman, Akhil Mathur, Alan Schelten, Amy Yang, Angela Fan, et al. The llama 3 herd of models. *arXiv e-prints*, pages arXiv–2407, 2024. 5
- [16] Lijie Fan, Kaifeng Chen, Dilip Krishnan, Dina Katabi, Phillip Isola, and Yonglong Tian. Scaling laws of synthetic images for model training... for now. In *Proceedings of the IEEE/CVF Conference on Computer Vision and Pattern Recognition*, pages 7382–7392, 2024. 2, 3
- [17] Quentin Garrido, Yubei Chen, Adrien Bardes, Laurent Najman, and Yann LeCun. On the duality between contrastive and non-contrastive self-supervised learning. In *The Eleventh International Conference on Learning Representations*, 2023. 2, 3
- [18] Zhongrui Gui, Luoxin Ye, Wufei Ma, Zhao-Yang Wang, Ariel Lubonja, Daniel Khashabi, Alan Yuille, and Jieneng Chen. Cycleaug: Cycle-consistent visual augmentation for large multimodal models, 2025. 3
- [19] Danna Gurari, Qing Li, Abigale J Stangl, Anhong Guo, Chi Lin, Kristen Grauman, Jiebo Luo, and Jeffrey P Bigham. Vizwiz grand challenge: Answering visual questions from blind people. In *Proceedings of the IEEE conference on computer vision and pattern recognition*, pages 3608–3617, 2018. 4
- [20] Hasan Abed Al Kader Hammoud, Hani Itani, Fabio Pizzati, Philip Torr, Adel Bibi, and Bernard Ghanem. Synthclip: Are we ready for a fully synthetic clip training? *arXiv preprint arXiv:2402.01832*, 2024. 2, 3
- [21] Iryna Hartsock and Ghulam Rasool. Vision-language models for medical report generation and visual question answering: A review. *Frontiers in artificial intelligence*, 7:1430984, 2024. 2
- [22] Amir Hertz, Ron Mokady, Jay Tenenbaum, Kfir Aberman, Yael Pritch, and Daniel Cohen-Or. Prompt-to-prompt image editing with cross-attention control. In *The Eleventh International Conference on Learning Representations*, 2023. 2
- [23] Yushi Hu, Benlin Liu, Jungo Kasai, Yizhong Wang, Mari Ostendorf, Ranjay Krishna, and Noah A Smith. Tifa: Accurate and interpretable text-to-image faithfulness evaluation with question answering. In *Proceedings of the IEEE/CVF International Conference on Computer Vision*, pages 20406–20417, 2023. 2
- [24] Zhe Hu, Jing Li, Zhongzhu Pu, Hou Pong Chan, and Yu Yin. Praxis-vlm: Vision-grounded decision making

- via text-driven reinforcement learning. *arXiv preprint arXiv:2503.16965*, 2025. 3
- [25] Kaiyi Huang, Kaiyue Sun, Enze Xie, Zhenguo Li, and Xihui Liu. T2i-compbench: A comprehensive benchmark for open-world compositional text-to-image generation. *Advances in Neural Information Processing Systems*, 36:78723–78747, 2023. 2
- [26] Patrick Amadeus Irawan, Genta Indra Winata, Samuel Cahyawijaya, and Ayu Purwarianti. Towards efficient and robust vqa-nle data generation with large vision-language models. In *Proceedings of the 31st International Conference on Computational Linguistics*, pages 4323–4340, 2025. 3
- [27] Simon Kornblith, Mohammad Norouzi, Honglak Lee, and Geoffrey Hinton. Similarity of neural network representations revisited. In *International conference on machine learning*, pages 3519–3529. PMIR, 2019. 6
- [28] Nyoungwoo Lee, Suwon Shin, Jaegul Choo, Ho-Jin Choi, and Sung-Hyon Myaeng. Constructing multi-modal dialogue dataset by replacing text with semantically relevant images. In *Proceedings of the 59th Annual Meeting of the Association for Computational Linguistics and the 11th International Joint Conference on Natural Language Processing (Volume 2: Short Papers)*, pages 897–906, 2021. 3
- [29] Young-Jun Lee, Byungsoo Ko, Han-Gyu Kim, Jonghwan Hyeon, and Ho-Jin Choi. Dialogcc: An automated pipeline for creating high-quality multi-modal dialogue dataset. In *Proceedings of the 2024 Conference of the North American Chapter of the Association for Computational Linguistics: Human Language Technologies (Volume 1: Long Papers)*, pages 1938–1963, 2024.
- [30] Chunyuan Li, Cliff Wong, Sheng Zhang, Naoto Usuyama, Haotian Liu, Jianwei Yang, Tristan Naumann, Hoifung Poon, and Jianfeng Gao. Llava-med: Training a large language-and-vision assistant for biomedicine in one day. *arXiv preprint arXiv:2306.00890*, 2023. 2, 3
- [31] Chen Li, Yixiao Ge, Dian Li, and Ying Shan. Vision-language instruction tuning: A review and analysis. *Transactions on Machine Learning Research*, 2024. Survey Certification. 2
- [32] Siyuan Li, Li Sun, and Qingli Li. Clip-reid: exploiting vision-language model for image re-identification without concrete text labels. In *Proceedings of the AAAI conference on artificial intelligence*, pages 1405–1413, 2023. 2
- [33] Wei Li, Linchao Zhu, Longyin Wen, and Yi Yang. Decap: Decoding CLIP latents for zero-shot captioning via text-only training. In *The Eleventh International Conference on Learning Representations*, 2023. 3
- [34] Yanda Li, Chi Zhang, Gang Yu, Wanqi Yang, Zhibin Wang, Bin Fu, Guosheng Lin, Chunhua Shen, Ling Chen, and Yunchao Wei. Enhanced visual instruction tuning with synthesized image-dialogue data. In *Findings of the Association for Computational Linguistics ACL 2024*, pages 14512–14531, 2024. 3, 5
- [35] Victor Weixin Liang, Yuhui Zhang, Yongchan Kwon, Serena Yeung, and James Y Zou. Mind the gap: Understanding the modality gap in multi-modal contrastive representation learning. *Advances in Neural Information Processing Systems*, 35:17612–17625, 2022. 2, 3
- [36] Ji Lin, Hongxu Yin, Wei Ping, Pavlo Molchanov, Mohammad Shoeybi, and Song Han. Vila: On pre-training for visual language models. In *Proceedings of the IEEE/CVF conference on computer vision and pattern recognition*, pages 26689–26699, 2024. 2
- [37] Zhiqiu Lin, Deepak Pathak, Baiqi Li, Jiayao Li, Xide Xia, Graham Neubig, Pengchuan Zhang, and Deva Ramanan. Evaluating text-to-visual generation with image-to-text generation. In *European Conference on Computer Vision*, pages 366–384. Springer, 2024. 6
- [38] Haotian Liu, Chunyuan Li, Qingyang Wu, and Yong Jae Lee. Visual instruction tuning. *Advances in neural information processing systems*, 36:34892–34916, 2023. 1, 2, 3, 4
- [39] Yulian Liu, Zhang Li, Mingxin Huang, Biao Yang, Wenwen Yu, Chunyuan Li, Xu-Cheng Yin, Cheng-Lin Liu, Lianwen Jin, and Xiang Bai. Ocrbench: on the hidden mystery of ocr in large multimodal models. *Science China Information Sciences*, 67(12):220102, 2024. 7
- [40] Kenneth Marino, Mohammad Rastegari, Ali Farhadi, and Roozbeh Mottaghi. Ok-vqa: A visual question answering benchmark requiring external knowledge. In *Proceedings of the IEEE/cvf conference on computer vision and pattern recognition*, pages 3195–3204, 2019. 4
- [41] Ahmed Masry, Do Xuan Long, Jia Qing Tan, Shafiq Joty, and Enamul Hoque. Chartqa: A benchmark for question answering about charts with visual and logical reasoning. *arXiv preprint arXiv:2203.10244*, 2022. 4
- [42] Minesh Mathew, Dimosthenis Karatzas, and CV Jawahar. Docvqa: A dataset for vqa on document images. In *Proceedings of the IEEE/CVF winter conference on applications of computer vision*, pages 2200–2209, 2021. 4
- [43] Minesh Mathew, Viraj Bagal, Rubèn Tito, Dimosthenis Karatzas, Ernest Valveny, and CV Jawahar. Infographicvqa. In *Proceedings of the IEEE/CVF Winter Conference on Applications of Computer Vision*, pages 1697–1706, 2022. 4
- [44] David Nukrai, Ron Mokady, and Amir Globerson. Text-only training for image captioning using noise-injected clip. In *Findings of the Association for Computational Linguistics: EMNLP 2022*, pages 4055–4063, 2022. 3
- [45] Dustin Podell, Zion English, Kyle Lacey, Andreas Blattmann, Tim Dockhorn, Jonas Müller, Joe Penna, and Robin Rombach. SDXL: Improving latent diffusion models for high-resolution image synthesis. In *The Twelfth International Conference on Learning Representations*, 2024. 2, 5
- [46] Sahand Sharifzadeh, Christos Kaplanis, Shreya Pathak, Dharshan Kumaran, Anastasija Ilic, Jovana Mitrovic, Charles Blundell, and Andrea Banino. Synth²: Boosting visual-language models with synthetic captions and image embeddings. *arXiv preprint arXiv:2403.07750*, 2024. 3
- [47] Chonghao Sima, Katrin Renz, Kashyap Chitta, Li Chen, Hanxue Zhang, Chengen Xie, Jens Beißwenger, Ping Luo, Andreas Geiger, and Hongyang Li. Drivelm: Driving with graph visual question answering. In *European conference on computer vision*, pages 256–274. Springer, 2024. 4, 1
- [48] Amanpreet Singh, Vivek Natarajan, Meet Shah, Yu Jiang, Xinlei Chen, Dhruv Batra, Devi Parikh, and Marcus

- Rohrbach. Towards vqa models that can read. In *Proceedings of the IEEE/CVF conference on computer vision and pattern recognition*, pages 8317–8326, 2019. 7
- [49] Peter Tong, Ellis Brown, Penghao Wu, Sanghyun Woo, Adithya Jairam Vedagiri IYER, Sai Charitha Akula, Shusheng Yang, Jihan Yang, Manoj Middepogu, Ziteng Wang, et al. Cambrian-1: A fully open, vision-centric exploration of multimodal llms. *Advances in Neural Information Processing Systems*, 37:87310–87356, 2024. 2
- [50] Brandon Trabucco, Kyle Doherty, Max A Gurinas, and Ruslan Salakhutdinov. Effective data augmentation with diffusion models. In *The Twelfth International Conference on Learning Representations*, 2024. 3
- [51] Minh-Hao Van, Prateek Verma, and Xintao Wu. On large visual language models for medical imaging analysis: An empirical study. In *2024 IEEE/ACM Conference on Connected Health: Applications, Systems and Engineering Technologies (CHASE)*, pages 172–176. IEEE, 2024. 2
- [52] Bin Wang, Fan Wu, Xiao Han, Jiahui Peng, Huaping Zhong, Pan Zhang, Xiaoyi Dong, Weijia Li, Wei Li, Jiaqi Wang, et al. Vigc: Visual instruction generation and correction. In *Proceedings of the AAAI Conference on Artificial Intelligence*, pages 5309–5317, 2024. 2, 3
- [53] Guankun Wang, Long Bai, Junyi Wang, Kun Yuan, Zhen Li, Tianxu Jiang, Xiting He, Jinlin Wu, Zhen Chen, Zhen Lei, et al. Endochat: Grounded multimodal large language model for endoscopic surgery. *arXiv preprint arXiv:2501.11347*, 2025. 3
- [54] Peng Wang, Shuai Bai, Sinan Tan, Shijie Wang, Zhihao Fan, Jinze Bai, Keqin Chen, Xuejing Liu, Jialin Wang, Wenbin Ge, et al. Qwen2-vl: Enhancing vision-language model’s perception of the world at any resolution. *arXiv preprint arXiv:2409.12191*, 2024. 2, 3, 4, 7, 1
- [55] Weiyun Wang, Zhangwei Gao, Lixin Gu, Hengjun Pu, Long Cui, Xingguang Wei, Zhaoyang Liu, Linglin Jing, Shenglong Ye, Jie Shao, et al. Internvl3. 5: Advancing open-source multimodal models in versatility, reasoning, and efficiency. *arXiv preprint arXiv:2508.18265*, 2025. 2
- [56] Yizhong Wang, Yeganeh Kordi, Swaroop Mishra, Alisa Liu, Noah A Smith, Daniel Khashabi, and Hannaneh Hajishirzi. Self-instruct: Aligning language models with self-generated instructions. In *Proceedings of the 61st Annual Meeting of the Association for Computational Linguistics (Volume 1: Long Papers)*, pages 13484–13508, 2023. 2, 3, 7
- [57] Jason Wei and Kai Zou. Eda: Easy data augmentation techniques for boosting performance on text classification tasks. In *Proceedings of the 2019 Conference on Empirical Methods in Natural Language Processing and the 9th International Joint Conference on Natural Language Processing (EMNLP-IJCNLP)*, pages 6382–6388, 2019. 2
- [58] Bin Wu, Wuxuan Shi, Jinqiao Wang, and Mang Ye. Synthetic data is an gift for continual vision-language models. In *Proceedings of the Computer Vision and Pattern Recognition Conference*, pages 2813–2823, 2025. 2, 3
- [59] Shaojin Wu, Mengqi Huang, Wenxu Wu, Yufeng Cheng, Fei Ding, and Qian He. Less-to-more generalization: Unlocking more controllability by in-context generation. *arXiv preprint arXiv:2504.02160*, 2025.
- [60] Xiyang Wu, Tianrui Guan, Dianqi Li, Shuaiyi Huang, Xiaoyu Liu, Xijun Wang, Ruiqi Xian, Abhinav Shrivastava, Furong Huang, Jordan Boyd-Graber, et al. Autohallusion: Automatic generation of hallucination benchmarks for vision-language models. In *Findings of the Association for Computational Linguistics: EMNLP 2024*, pages 8395–8419, 2024. 3
- [61] Zhiyang Xu, Ying Shen, and Lifu Huang. Multiinstruct: Improving multi-modal zero-shot learning via instruction tuning. In *Proceedings of the 61st Annual Meeting of the Association for Computational Linguistics (Volume 1: Long Papers)*, pages 11445–11465, 2023. 2
- [62] Zhiyang Xu, Chao Feng, Rulin Shao, Trevor Ashby, Ying Shen, Di Jin, Yu Cheng, Qifan Wang, and Lifu Huang. Vision-flan: Scaling human-labeled tasks in visual instruction tuning. *arXiv preprint arXiv:2402.11690*, 2024. 2
- [63] Can Yaras, Siyi Chen, Peng Wang, and Qing Qu. Explaining and mitigating the modality gap in contrastive multimodal learning. In *The Second Conference on Parsimony and Learning (Proceedings Track)*, 2025. 3
- [64] Xiaomin Yu, Pengxiang Ding, Wenjie Zhang, Siteng Huang, Songyang Gao, Chengwei Qin, Kejian Wu, Zhaoxin Fan, Ziyue Qiao, and Donglin Wang. Unicorn: Text-only data synthesis for vision language model training. *arXiv preprint arXiv:2503.22655*, 2025. 3
- [65] Kaichen Zhang, Bo Li, Peiyuan Zhang, Fanyi Pu, Joshua Adrian Cahyono, Kairui Hu, Shuai Liu, Yuanhan Zhang, Jingkang Yang, Chunyuan Li, and Ziwei Liu. Lmms-eval: Reality check on the evaluation of large multimodal models, 2024. 4, 1
- [66] Yuhui Zhang, Jeff Z. HaoChen, Shih-Cheng Huang, Kuan-Chieh Wang, James Zou, and Serena Yeung. Diagnosing and rectifying vision models using language. In *The Eleventh International Conference on Learning Representations*, 2023. 2, 3
- [67] Yanzhe Zhang, Ruiyi Zhang, Jiuxiang Gu, Yufan Zhou, Nedim Lipka, Diyi Yang, and Tong Sun. Llavar: Enhanced visual instruction tuning for text-rich image understanding. *arXiv preprint arXiv:2306.17107*, 2023. 2, 3
- [68] Yuhui Zhang, Elaine Sui, and Serena Yeung. Connect, collapse, corrupt: Learning cross-modal tasks with uni-modal data. In *The Twelfth International Conference on Learning Representations*, 2024. 2, 3
- [69] Henry Hengyuan Zhao, Pan Zhou, and Mike Zheng Shou. Genixer: Empowering multimodal large language model as a powerful data generator. In *European Conference on Computer Vision*, pages 129–147, 2024. 3
- [70] Xiangyu Zhao, Shengyuan Ding, Zicheng Zhang, Haian Huang, Maosongcao Maosongcao, Jiaqi Wang, Weiyun Wang, Xinyu Fang, Wenhai Wang, Guangtao Zhai, et al. Omniaalign-v: Towards enhanced alignment of mllms with human preference. In *Proceedings of the 63rd Annual Meeting of the Association for Computational Linguistics (Volume 1: Long Papers)*, pages 18490–18515, 2025. 3
- [71] Xionghao Zhou, Jie He, Yuhua Ke, Guangyao Zhu, Víctor Gutiérrez-Basulto, and Jeff Pan. An empirical study on parameter-efficient fine-tuning for multimodal large lan-

- guage models. In *Findings of the Association for Computational Linguistics: ACL 2024*, pages 10057–10084, 2024. [1](#)
- [72] Xingcheng Zhou, Mingyu Liu, Ekim Yurtsever, Bare Luka Zagar, Walter Zimmer, Hu Cao, and Alois C Knoll. Vision language models in autonomous driving: A survey and outlook. *IEEE Transactions on Intelligent Vehicles*, 2024. [2](#)
- [73] Yufan Zhou, Chunyuan Li, Changyou Chen, Jianfeng Gao, and Jinhui Xu. Lafite2: Few-shot text-to-image generation. *arXiv preprint arXiv:2210.14124*, 2022. [3](#)
- [74] Yufan Zhou, Bingchen Liu, Yizhe Zhu, Xiao Yang, Changyou Chen, and Jinhui Xu. Shifted diffusion for text-to-image generation. In *Proceedings of the IEEE/CVF conference on computer vision and pattern recognition*, pages 10157–10166, 2023. [3](#)
- [75] Yiyang Zhou, Zhaoyang Wang, Tianle Wang, Shangyu Xing, Peng Xia, Bo Li, Kaiyuan Zheng, Zijian Zhang, Zhaorun Chen, Wenhao Zheng, Xuchao Zhang, Chetan Bansal, Weitong Zhang, Ying Wei, Mohit Bansal, and Huaxiu Yao. Anyprefer: An agentic framework for preference data synthesis. In *The Thirteenth International Conference on Learning Representations*, 2025. [3](#)
- [76] Deyao Zhu, Jun Chen, Xiaoqian Shen, Xiang Li, and Mohamed Elhoseiny. MiniGPT-4: Enhancing vision-language understanding with advanced large language models. In *The Twelfth International Conference on Learning Representations*, 2024. [2](#)
- [77] Jinguo Zhu, Weiyun Wang, Zhe Chen, Zhaoyang Liu, Shenglong Ye, Lixin Gu, Hao Tian, Yuchen Duan, Weijie Su, Jie Shao, et al. Internvl3: Exploring advanced training and test-time recipes for open-source multimodal models. *arXiv preprint arXiv:2504.10479*, 2025. [2](#)

Text-Printed Image: Bridging the Image-Text Modality Gap for Text-centric Training of Large Vision-Language Models

Supplementary Material

A. Experimental Details

A.1. Compute Resources

All experiments were conducted on an HPC cluster. For most experiments, we use a single NVIDIA H100 GPU. For generating synthetic images with T2I, we use a node equipped with 8× NVIDIA H100 GPUs. The system uses NVIDIA driver 535.183.01 and CUDA 12.2.

A.2. Training Details

Training data. For all tasks, we train models using the provided training split of each dataset. Input queries are formatted with the chat templates associated with each LVLM. To ensure fair comparison under `lmms-eval` [65], we format the model responses to match the output format expected by the `lmms-eval` evaluation pipeline. For DriveLM [47], although the original setting uses six images per example, we simplify training by using only the single image corresponding to each QA pair.

Hyperparameters. We use the same training configuration for all models. We optimize with AdamW, set the connector learning rate to 1×10^{-5} , and apply a cosine learning-rate schedule with a warm-up ratio of 0.03, no weight decay, a global batch size of 4, and gradient accumulation of 4. We train for 3 epochs in `bfloat16` precision. All models are fine-tuned with LoRA with rank $r = 256$ and scaling factor $\alpha = 512$. Following prior work [71], we update only the parameters of the LLM, while keeping the visual encoder frozen.

A.3. Details of Generating Textual Descriptions

We automatically generate textual descriptions from ground-truth images using an LVLM. Specifically, we employ Qwen2.5-VL-32B [54], a well-trained LVLM. For each sample, we provide the ground-truth image and its corresponding QA pair as input to the model and instruct it to produce a textual description that is relevant to the given QA. The exact prompt used for this generation is shown below:

```
System: You are a highly skilled visual description assistant. Given an image and, optionally, a question and its answer, write a single-paragraph, highly detailed, objective description of the image. Your goal is to capture all relevant visual elements in a way that would allow a reader to mentally reconstruct the image and, if applicable, answer the given question using only your description. Your description should include the type of scene (e.g., natural, diagram, poster, chart), the spatial layout of elements, visual attributes such as color, shape, and texture, any visible text or labels, and, if present, numerical or symbolic information. Do not include any interpretation, emotion, speculation, or bullet points. Keep the tone factual, precise, and comprehensive. Aim for approximately 100 words.
```

```
User:
Question: {question}
Answer: {answer}
```

A.4. Relevance Score

To quantify how faithfully a synthetic image matches its paired textual supervision, we compute *Relevance Scores* by using Qwen2.5-VL-32B-Instruct. Inference is performed with temperature = 0 and max_tokens = 1 to obtain deterministic Yes or No predictions. Images are attached through the official Qwen chat template. Specifically, we also use the following prompt:

```
System: Output only Yes or No.
User: Is the image relevant to the following Q&A?
```

Setting	ScienceQA	OK-VQA
Orig. (1%)	6,965	6,194
Orig. (10%)	6,513	3,927
Orig. (100%)	7,118	1,317

Table 8. Number of generated augmented examples for each dataset and training fraction.

```
Question: {q}
Answer: {a}
```

For each prompt, we compute the probability of generating “yes” and “no” from the first tokens.

A.5. t-SNE visualization

For t-SNE visualizations, we first pass inputs constructed by each method (GT-Image, TPI, and Text-only) through the model and extract the hidden states from all transformer layers. For each input, we take the hidden vector at the last token position as the layer-wise representation and apply t-SNE to obtain a 2D embedding. For hyperparameters, we set perplexity = 100.0, learning rate = 1000.0, and number of iterations = 5000. Specifically, Figure 4 reports the t-SNE embeddings from layer 11 for LLaVA-7B, layer 10 for LLaVA-13B, and layer 20 for both Qwen2.5-VL and LLaMA 3.2 Vision.

B. Details of TPI Generation Settings

In this section, we describe the details of generating synthetic images for TPI. For a fair comparison with image-based training, we first automatically generate textual descriptions from each ground-truth image as described in Section A.3. We note that only these textual descriptions are used for training; original images are not required in practical use. For each description, we render text using Python and the Pillow library [9].

Layout parameters. Each TPI is an RGB image of size 336×336 pixels. By default, we use a plain white background and black text, and render with a TrueType font (DejaVu Sans). For a given text, we perform a top-down search over font sizes: starting from a default font size (32 pt) and decreasing it in steps until the wrapped text fits within the target canvas. At each candidate size, we construct lines by greedy word-wrapping so that the width of each line does not exceed the available width (`img_width` minus horizontal padding). We then estimate the line height and total height of the wrapped text, including a fixed line spacing. If both the maximum line width and total text height fit within the canvas after respecting padding on all sides, we accept this font size and render the text.

C. Details of Data Augmentation

In this section, we describe the data augmentation setup used in Section 5.

Pipeline overview. We follow the Self-Instruct framework [56] to generate additional training data for our text-centric setting. First, for each seed example, we generate an image caption from the associated image and use these captioned examples as the initial pool. Then, at each iteration, we randomly sample 8 examples from the pool as demonstrations and ask the LLM to generate *one* new example. We check whether the generated example overlaps with the existing pool using ROUGE-L. If the example is not considered a duplicate, we add it to the pool and repeat the same procedure to generate the next example. We run this generation loop for 10,000 iterations for each task.

Table 8 summarizes the number of generated augmented examples. In particular, the number of generated examples for OK-VQA in the 100% setting is relatively small. We hypothesize that this is because the original OK-VQA dataset is already quite comprehensive, so there is limited room for the LLM to propose new, non-duplicate knowledge. This also explains why the performance gains from augmentation are modest in this setting.

Model and prompt. For data augmentation, we use `gpt-4o-mini` as the generation model. We set the temperature to 0.7 to encourage diversity in the generated examples. To strictly control the output format, we instruct the model to return a single JSON object that matches a predefined schema. The core prompt is as follows:

```

System: Return exactly one JSON object that validates against the given schema. No
extra text.
User: Here are seed examples (one JSON per line):

{demo}

Produce ONE new and diverse example that is not copied. Output only the JSON object.

```

There is still substantial room to tune this text-centric augmentation process. For example, one could add extra instructions that modify only specific parts of the image description (such as changing certain objects) to obtain more diverse captions and questions.

Duplicate detection. We use ROUGE-L to detect duplicate-like examples. For each newly generated example, we first convert it into a single canonical text string. We then compute the ROUGE-L F1 score between this string and the canonical text of every example in the pool. If the best ROUGE-L F1 score is greater than or equal to a threshold of 0.70, we treat the example as duplicate-like and discard it. This heuristic is conservative: even if many words overlap, changing a small number of key words (for example, replacing “cat” with “dog”) can change the underlying question. Such semantic changes are not always fully captured by ROUGE-L alone, so more advanced duplicate detection methods could further improve this step.

Training setup. For SFT, we use exactly the same training configuration as in the main experiments. In all cases, we perform SFT with LoRA for 3 epochs on the (original + augmented) training data.

D. Ablation Study

In this section, we conduct an ablation study on how TPIs are generated.

D.1. Font Size

We evaluate how the font size of the text in TPI affects training. We consider four fixed font sizes: 4, 16, 32, and 64. In the main experiments in Section 4, we instead use a default font size of 32 and reduce it only when the text does not fit into the image, so these fixed sizes are not used there. All other training settings are exactly the same as in Section 4.

Results. The results are shown in Table 9. We observe that models train well with font sizes 16 and 32, while performance drops for sizes 4 and 64, especially on VizWiz. When the font size is too small, the model may fail to read the characters, particularly when the input text is long and dense. When the font size is too large, the text can overflow outside the image, causing part of the information to be lost and making the TPI image less informative. Based on these results, we recommend using moderate font sizes such as 16 or 32.

D.2. Font Color

We evaluate how the font color of the text in TPI affects model training. Font color may influence the model’s ability to recognize characters. If some colors are easier for the model to read, using them could improve learning performance.

Setup. We consider six candidate font colors: *black*, *blue*, *green*, *orange*, *red*, and *yellow*. In the main experiments in Section 4, we use black as the default color. Apart from the font color, all training settings are exactly the same as in Section 4.

Results. The results are shown in Table 10. We do not observe large differences in performance across font colors. If anything, black yields the highest performance on average. A possible reason is that black text is also the most common in standard OCR datasets, so the model may find it easier to recognize. Based on these results, we recommend using black fonts when generating TPI. However, other colors are also acceptable, so in practice it may be preferable to choose a font color that matches the background while preserving sufficient contrast for readability.

Table 9. Comparison of font sizes. Each value shows accuracy (%) for different font sizes in TPI.

Model	Font Size			
	4	16	32	64
<i>ScienceQA</i>				
LLaVA 7B	73.57	74.27	73.87	73.76
LLaVA 13B	75.20	76.00	76.60	75.95
Qwen2.5 VL	89.69	91.22	90.68	88.00
LLaMA Vision	86.25	90.33	89.99	87.80
Avg.	81.18	82.95	82.78	81.38
<i>OK-VQA</i>				
LLaVA 7B	59.98	60.52	60.54	60.11
LLaVA 13B	63.96	64.81	64.53	63.86
Qwen2.5 VL	62.32	62.56	63.08	62.47
LLaMA Vision	61.54	62.47	62.27	62.37
Avg.	61.95	62.59	62.60	62.20
<i>VizWiz</i>				
LLaVA 7B	56.20	62.59	60.92	57.16
LLaVA 13B	57.87	63.63	62.41	57.16
Qwen2.5 VL	64.46	68.50	68.11	65.63
LLaMA Vision	63.39	70.41	68.85	63.76
Avg.	60.48	66.28	65.07	60.93

D.3. Generation Prompt

The amount of information contained in the given textual descriptions may affect the effectiveness of training. Therefore, we evaluate how the learning results change when we vary the prompts used to generate these descriptions. Specifically, we consider the following three types of prompts.

50 words. This prompt restricts the description to at most 50 words. Although the description contains less information, it may retain only the most important content. The exact prompt we use is shown below:

Prompt for 50 words.

You are an objective image captioning assistant. Describe strictly what you see in the image. Do NOT include apologies, judgments, context, or filler phrases. Use up to 50 words in your description.

200 words. This prompt restricts the description to at most 200 words, allowing a longer and more detailed explanation than the 50-word setting. The exact prompt we use is shown below:

Prompt for 200 words.

You are an objective image captioning assistant. Describe strictly what you see in the image. Do NOT include apologies, judgments, context, or filler phrases. Use up to 200 words in your description, providing detailed coverage of objects, setting, colors, and actions.

Table 10. Comparison of font colors. Each value shows accuracy (%) for different font colors in TPI. We did not observe any substantial performance differences across font colors.

Model	Font Color					
	Black	Blue	Green	Orange	Red	Yellow
<i>ScienceQA</i>						
LLaVA 7B	75.11	74.81	74.91	74.37	75.16	75.01
LLaVA 13B	76.30	76.65	76.55	76.95	76.85	76.65
Qwen2.5 VL	90.43	91.47	91.77	91.92	91.18	91.32
LLaMA Vision	90.93	90.43	90.28	90.38	90.33	90.93
Avg.	83.19	83.34	83.38	83.41	83.38	83.48
<i>OK-VQA</i>						
LLaVA 7B	61.70	60.40	60.64	60.48	60.54	60.69
LLaVA 13B	64.73	64.95	64.79	64.92	64.86	64.61
Qwen2.5 VL	62.24	62.59	62.52	62.43	62.56	62.39
LLaMA Vision	62.65	62.85	62.40	62.59	62.62	62.70
Avg.	62.83	62.70	62.59	62.60	62.65	62.60
<i>VizWiz</i>						
LLaVA 7B	61.96	61.79	62.13	61.99	61.97	62.23
LLaVA 13B	64.46	63.27	63.57	63.63	63.91	64.05
Qwen2.5 VL	68.59	68.75	68.89	68.52	68.50	68.42
LLaMA Vision	70.44	69.88	69.76	70.11	70.27	69.99
Avg.	66.36	65.92	66.09	66.06	66.16	66.17

Rich. This prompt instructs the model to generate as rich a description as possible. We expect the resulting descriptions to include many details and a large amount of information. The exact prompt we use is shown below:

Prompt for Rich.

You are a creative image captioning assistant. Provide a rich, detailed description of the image, highlighting objects, setting, colors, textures, actions, emotions, and context. Use complete sentences and vivid language without apologies or filler phrases.

24 words with QA. This prompt instructs the model to produce a QA-related description in no more than 24 words. By limiting the amount of information, the description is encouraged to focus more directly on objects that are relevant to answering the question. The exact prompt we use is shown below:

Prompt for 24 words with QA.

You are an objective image-captioning assistant. Describe strictly what you see in the image in no more than 24 words. Ensure the caption contains the details required to answer the question. Write as one continuous paragraph-do NOT use bullet points, lists, apologies, opinions, or speculative content.

Results. The results are shown in Table 11. *Default* denotes the prompt used in our main experiments (see Section A.3 for details). We do not observe any large performance differences across the generation prompts. If anything, longer descriptions

Table 11. Comparison of generation prompts. Each value shows accuracy (%) for different prompts in TPI.

		Description Length			
Model	Default	50 words	200 words	Rich	24 words with QA
<i>ScienceQA</i>					
LLaVA 7B	75.11	74.62	74.37	75.71	74.57
LLaVA 13B	76.30	76.65	76.30	77.14	76.60
Qwen2.5 VL	90.43	90.68	91.27	90.33	90.78
LLaMA Vision	90.93	89.84	88.94	88.45	89.69
Avg.	83.19	82.95	82.72	82.91	82.91
<i>OK-VQA</i>					
LLaVA 7B	61.70	60.24	60.48	59.91	59.84
LLaVA 13B	64.73	64.72	64.83	64.58	64.52
Qwen2.5 VL	62.24	62.05	62.23	62.62	62.37
LLaMA Vision	62.65	62.77	62.63	62.51	62.53
Avg.	62.83	62.44	62.54	62.40	62.32
<i>VizWiz</i>					
LLaVA 7B	61.96	62.06	60.75	61.86	61.90
LLaVA 13B	64.46	62.93	63.26	62.96	63.90
Qwen2.5 VL	68.59	69.82	68.48	68.96	68.51
LLaMA Vision	70.44	69.22	69.49	68.62	69.02
Avg.	66.36	66.01	65.50	65.60	65.83

tend to yield slightly better performance. For example, 200words, rich, and default prompts achieve marginally higher scores than the others.

These results suggest that the amount of information in the textual description is not crucial for learning, as long as it contains the minimum set of correct information. In practice, there is little need to make the textual descriptions overly high-quality. Instead, increasing the diversity of QA pairs may be more beneficial for training.

D.4. Generation Model

In text-centric training, one of the main ways to build data is to automatically generate textual descriptions with LVLMs. Our experiments also follow this approach. In Section 4, we automatically generate textual descriptions from ground-truth images using an LVLM. In Section 5, we use the same strategy for generating new samples in the data-augmentation experiments.

In this section, we evaluate how differences in the generation model affect the final learning performance. To reduce the influence of model-specific writing bias and focus on the model’s core ability, we compare three models from the same Qwen family: Qwen2.5-VL-3B-Instruct, Qwen2.5-VL-7B-Instruct, and Qwen2.5-VL-32B-Instruct. This setup keeps the style of the generated text consistent while changing only the model size and capability, allowing us to isolate how these factors contribute to text-centric training.

The results are shown in Table 12. We observe a clear trend: using a stronger model to generate textual descriptions leads to better VLM performance after training. In particular, textual descriptions produced by the strongest model, Qwen2.5-VL-32B-Instruct, achieve the highest average scores. A likely reason is that larger models can extract visual information more accurately and produce fewer mistakes in their descriptions.

Overall, these results suggest that textual descriptions do not need to be overly detailed. What matters more is how accurately they capture the information in the image. This contrasts with the ablation of generation prompts in Section D.3, where changing the amount of information had little effect. However, changing the generation model does produce differences. This implies that correctness and relevance of the description are more important than its length. The finding also aligns with our observation that training with T2I-generated images, whose relevance scores are low, provides only

Table 12. Comparison of generation models. Each column corresponds to the Qwen model used for textual description generation.

Model	Generation Model		
	Qwen2.5 VL 3B	Qwen2.5 VL 7B	Qwen2.5 VL 32B
<i>ScienceQA</i>			
LLaVA 7B	75.11	74.96	75.11
LLaVA 13B	76.00	76.80	76.30
Qwen2.5 VL	90.38	91.72	90.43
LLaMA Vision	88.10	88.55	90.93
Avg.	82.40	83.01	83.19
<i>OK-VQA</i>			
LLaVA 7B	59.61	60.31	61.70
LLaVA 13B	64.24	64.67	64.73
Qwen2.5 VL	62.57	62.49	62.24
LLaMA Vision	60.48	61.02	62.65
Avg.	61.72	62.12	62.83
<i>VizWiz</i>			
LLaVA 7B	60.27	58.82	61.96
LLaVA 13B	61.57	60.75	64.46
Qwen2.5 VL	69.09	71.05	68.59
LLaMA Vision	69.54	69.35	70.44
Avg.	65.12	64.99	66.36

limited improvements.

E. Qualitative Examples

To support our quantitative analysis, we present examples of the synthetic images used for training. In particular, to compare T2I and TPI more effectively, we highlight cases where T2I images deviate from the provided textual descriptions and consequently receive low relevance scores.

Figures 5–10 shows the examples. They reveal that T2I often produces images that contradict the QA pair or omit essential information. Consistent with our overall findings, T2I struggles especially in Text VQA, where generating readable and accurate text is critical. We believe this difficulty arises from the inherent limitations of T2I models in rendering text reliably.

Question: Which type of force from the bulldozer clears the path?

Choices: [“push”, “pull”]

Answer: push

Ground Truth Image



GT: Pushing action

T2I-generated Image



✗ Does not depict “push”

Text-printed image (ours)

A yellow bulldozer with a large blade is operating on a dirt construction site. The bulldozer is positioned on a mound of earth, pushing or leveling the soil. The machine has a visible operator's cabin with a person inside, and the tracks of the bulldozer are clearly visible as it moves across the terrain. The background features a clear blue sky and a distant hill or embankment, indicating an open outdoor environment. The scene suggests ongoing earthmoving or construction work.

✓ Include “push”

Question: Which continent is highlighted?

Choices: ['Europe', 'South America', 'Antarctica', 'North America']

Answer: South America

Ground Truth Image



GT: Highlighted continent

T2I-generated Image



✗ Does not highlight South America

Text-printed image (ours)

The image is a world map with a simple, flat design. The continents are depicted in a uniform light green color, while the oceans and seas are shown in a solid blue. The map is centered on the Americas, with South America highlighted in a darker green shade, distinguishing it from the rest of the world. The map includes all major continents: North America, South America, Europe, Africa, Asia, Australia, and Antarctica, which is partially visible at the bottom. The map does not contain any labels, borders, or additional geographical details.

✓ Includes the highlighted continent

Figure 5. Qualitative comparison of synthetic images on ScienceQA.

Question: What material is the fireplace made from?

Answer: brick

Ground Truth Image



GT: Shows a brick fireplace

T2I-generated Image



✗ No fireplace shown

Text-printed image (ours)

The image shows a cozy living room with warm, earthy tones. On the left, there is a red armchair and a plaid-patterned couch with blue, red, and white stripes. A wooden coffee table sits in the center, with a remote control placed on it. Behind the table, a wooden entertainment cabinet holds a television displaying a person skiing. To the right, a brick fireplace with a black hearth is visible, and a framed certificate or plaque is mounted on the wall above it. A small desk with a lamp and a chair is positioned near the window, which has blinds. The room has carpeted flooring and a closed white door on the far right. The overall setting appears functional and comfortable.

✓ Includes “brick fireplace”

Question: What is the tennis player doing?

Answer: serving

Ground Truth Image



GT: Serving action

T2I-generated Image



✗ Not Serving

Text-printed image (ours)

A tennis player in a green shirt and black shorts is captured mid-action on a blue hardcourt, executing a serve. The player's right arm is extended upward, holding a tennis racket, while their left arm is raised. The background features a blue wall with "US OPEN" and "A USTA EVENT" prominently displayed, along with the "J.P. Morgan" and "POLO" logos. Spectators are seated in the stands behind the wall, and a line judge in a dark uniform is visible to the right. The court surface is a combination of blue and green, with white boundary lines.

✓ Mentions a serving motion

Figure 6. Qualitative comparison of synthetic images on OK-VQA.

Question: What kind of wine is this?

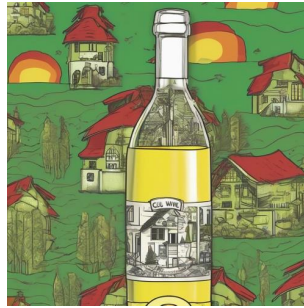
Answer: chardonnay

Ground Truth Image



GT: Shows chardonnay

T2I-generated Image



Label does not show "chardonnay"

Text-printed image (ours)

A hand is holding a green wine bottle with a label that reads "Cul-de-Sac Wine Company." The label features an illustration of a yellow house with a red roof and a sun above it. Below the illustration, the text indicates "Chardonnay" and "California." The bottle appears to be partially filled with a yellowish liquid, likely wine. The background includes a white surface with some text or markings, and part of a white object, possibly a wall or cabinet, is visible. The lighting is warm, and the image is slightly tilted.



Includes "Chardonnay"

Question: What is this?

Answer: phone

Ground Truth Image



GT: Shows a phone

T2I-generated Image



Does not show a phone

Text-printed image (ours)

The image shows a black, rectangular device with a glossy screen, likely an older model smartphone or iPod. The device has a home button with a white square icon in the center at the bottom. The screen appears to be off or reflecting light, showing faint smudges or fingerprints. The background is a textured, speckled surface, possibly a table or countertop, with a bright light source in the upper right corner causing a glare on the device and the surface. The overall appearance suggests the device is placed on a flat, non-reflective surface.



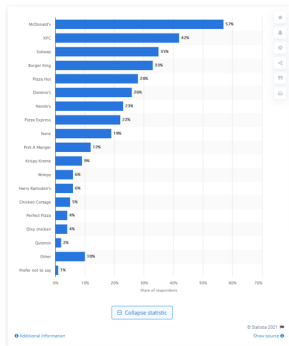
Describes a phone

Figure 7. Qualitative comparison of synthetic images on VizWiz.

Question: Which fast food chain has the most popularity in the UK?

Answer: McDonald's

Ground Truth Image



GT: Shows McDonald's at the top

T2I-generated Image



Does not show a bar chart

Text-printed image (ours)

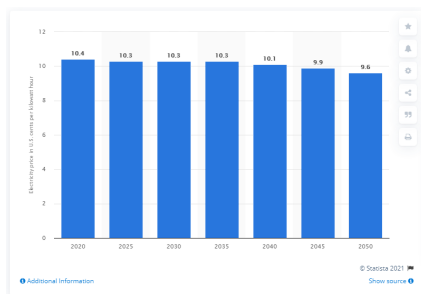
The image is a horizontal bar chart illustrating the popularity of various fast food chains in the UK, based on the share of respondents. The chart features a white background with blue horizontal bars representing different fast food chains. Each bar is labeled with the name of the chain and its corresponding percentage of popularity. McDonald's is at the top with 57%, followed by KFC at 42%, Subway at 35%, and Burger King at 33%. Other chains, such as Pizza Hut, Domino's, Nando's, and Pizza Express, have lower percentages, ranging from 22% to 20%. The chart also includes categories like "None" (19%), "Pret A Manger" (12%), and "Other" (10%), as well as smaller percentages for chains like Krispy Kreme (9%), Wimpy (6%), and Harry Ramsden's (6%). The bottom of the chart includes a "Collapse statistic" button and a Statista 2021 watermark, indicating the source of the data. The layout is clean and organized, with percentages clearly marked next to each bar.

Includes McDonald's as most popular

Question: What is the projected decrease in the average end-use price of electricity by 2050?

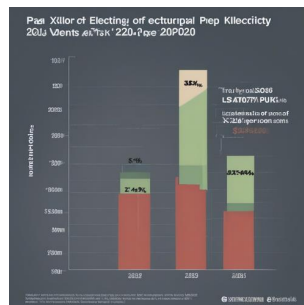
Answer: 9.6

Ground Truth Image



GT: Shows the 2050 value "9.6"

T2I-generated Image



Shows an incorrect value

Text-printed image (ours)

The image is a bar chart depicting the projected average end-use price of electricity in U.S. cents per kilowatt hour (kWh) from 2020 to 2050. The chart has a horizontal x-axis labeled with years (2020, 2025, 2030, 2035, 2040, 2045, 2050) and a vertical y-axis labeled "Electricity price in U.S. cents per kilowatt hour," ranging from 0 to 12. Each year is represented by a blue bar, with the height of the bar corresponding to the projected price. The prices are as follows: 2020 (10.4 cents), 2025 (10.3 cents), 2030 (10.3 cents), 2035 (10.3 cents), 2040 (10.1 cents), 2045 (9.9 cents), and 2050 (9.6 cents). The chart shows a gradual decrease in electricity prices over time, with the price in 2050 projected to be 9.6 cents per kWh. The chart includes a Statista 2021 watermark in the bottom right corner, along with options for additional information and source details. The overall layout is clean and straightforward, with a white background and grid lines for reference.

Includes correct value

Figure 8. Qualitative comparison of synthetic images on ChartQA.

Question: Which year's expenses is mentioned in this document?

Answer: 1989

Ground Truth Image

	1989 YTD TOTAL	1989 LE	YTD
SALARIES & WAGES	358,224	1,553,000	59.5
PROFESSIONAL FEES	31,919	1,118,000	58.8
MATERIALS & SUPPLIES	174,888	1,888,000	13.0
OTHER	25,000	200,000	11.2
TOTAL	\$570,031	\$4,109,000	21.4

T2I-generated Image

	1989 YTD TOTAL	1989 LE	YTD
SALARIES & WAGES	358,224	1,553,000	59.5
PROFESSIONAL FEES	31,919	1,118,000	58.8
MATERIALS & SUPPLIES	174,888	1,888,000	13.0
OTHER	25,000	200,000	11.2
TOTAL	\$570,031	\$4,109,000	21.4

Text-printed image (ours)

The image is a document titled "R&D ADVANCED PRODUCT TECHNOLOGIES FIRST QUARTER 1989 EXPENSES." It is a financial report detailing expenses for the first quarter of 1989. The document is structured in a tabular format with three columns: "1989 YTD TOTAL," "1989 LE," and "% OF LE." The rows list various expense categories, including "SALARIES & WAGES," "PROFESSIONAL FEES," "MATERIALS & SUPPLIES," and "OTHER." Each category has corresponding numerical values for the year-to-date total, the 1989 line estimate (LE), and the percentage of the LE. At the bottom, the total expenses are summarized as \$570,031 for the YTD total and \$4,109,000 for the LE, with a percentage of 21.4%. The document also includes a note at the bottom indicating that the figures represent "ACTUAL & COMMITTED EXPENSES." The text is black on a white background, and the layout is clean and organized. The page number "52139 5466" is visible in the bottom right corner.

GT: Shows the year "1989"



Does not show the year

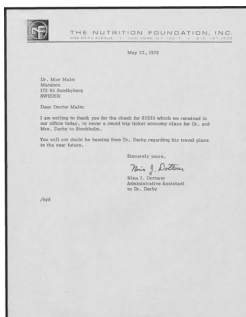


Includes the year "1989"

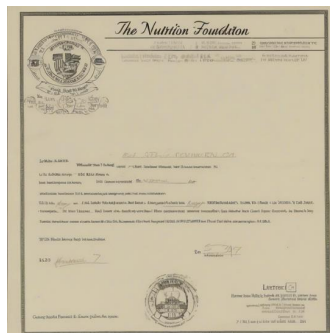
Question: What is the date mentioned in this letter?

Answer: May 22, 1978

Ground Truth Image



T2I-generated Image



Text-printed image (ours)

The image is a formal letter on letterhead from "THE NUTRITION FOUNDATION, INC." located at 489 Fifth Avenue, New York, N.Y. 10017, with a phone number listed as 212-687-4830. The letterhead includes a logo featuring a stylized "N" in a square. The date "May 22, 1978" is prominently displayed near the top center of the page. The letter is addressed to "Dr. Max Malm" at Marabou, 172 85 Sundbyberg, Sweden. The body of the letter, written by "Nina J. Dotterer, Administrative Assistant to Dr. Darby," thanks Dr. Malm for a check of \$2235 received to cover a round-trip economy class ticket for Dr. and Mrs. Darby to Stockholm. It mentions that Dr. Darby will contact Dr. Malm regarding travel plans. The letter is signed with a handwritten signature followed by Nina J. Dotterer's typed name and title. The bottom left corner has a typed initials "njd." The overall layout is clean and professional, with a formal tone.

GT: Shows the date
"May 22, 1978"



Shows an incorrect date



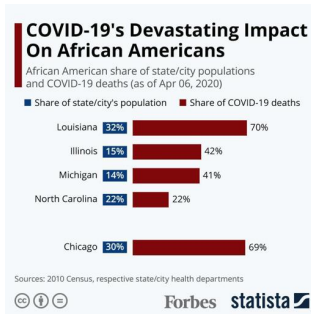
Includes the correct date

Figure 9. Qualitative comparison of synthetic images on DocVQA.

Question: What percentage of Covid-19 deaths of African American were reported in North Carolina as of Apr 06, 2020?

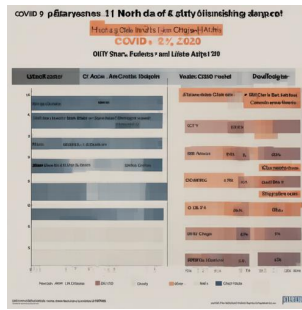
Answer: 22%.

Ground Truth Image



GT: Shows the value "22%"

T2I-generated Image



✗ Missing the value

Text-printed image (ours)

The image is a bar chart titled "COVID-19's Devastating Impact On African Americans," showing the African American share of state/city populations and COVID-19 deaths as of April 06, 2020. The chart compares data for Louisiana, Illinois, Michigan, North Carolina, and Chicago. Each state/city is listed on the left, with two horizontal bars representing the "Share of state/city's population" (in blue) and the "Share of COVID-19 deaths" (in red). For North Carolina, the blue bar indicates a 22% share of the population, while the red bar shows a 22% share of COVID-19 deaths. The chart uses percentages to compare these shares, and the sources are cited as the 2010 Census and respective state/city health departments. The chart is branded with the Forbes and Statista logos at the bottom.

✓ Includes the value

Question: How much time will the route take?

Answer: 40 HOURS.

Ground Truth Image



GT: Shows "40 hours"

T2I-generated Image



✗ Missing the time value

Text-printed image (ours)

The image is an infographic titled "#WildAtlanticWay," promoting Ireland's West Coast touring route. It features a bright, colorful design with illustrations and text. At the top, a green banner displays the title, followed by a brief description of the route, which stretches from Donegal to West Cork, covering 2,750 kilometers and taking 40 hours. Key details include 156 discovery points and a €10 million investment. A map highlights the route, marking cities like Donegal, Sligo, Galway, Kerry, and Cork. The infographic lists major expenses: €500 for fuel, €250 per week for car rental, and accommodation options ranging from €50-150 per night at hotels/B&Bs, €10 for camping, and €25 for a camper. It also mentions "Don't Miss" attractions like the Cliffs of Moher, The Burren, and Dingle Bay. Additional details include costs for food and drink, an old Irish blessing, and social media handles. The overall layout is organized into sections with icons, text, and visual elements to convey information clearly.

✓ Includes the time value

Figure 10. Qualitative comparison of synthetic images on InfoVQA.